

Synthesis and structure–activity relationships of metal–ligand complexes that potently inhibit cell migration

Anwar B. Beshir, Sankar K. Guchhait,[†] José A. Gascón and Gabriel Fenteany*

Department of Chemistry, University of Connecticut, Storrs, CT 06269, USA

Received 29 September 2007; revised 23 November 2007; accepted 27 November 2007

Available online 3 December 2007

Abstract—We screened the National Cancer Institute Diversity Set compound collection for small molecules that affect mammalian cell migration and identified NSC 295642 as an inhibitor of cell motility with nanomolar potency. We found by LC–MS and X-ray crystallography that NSC 295642, a Cu(II) complex of the Schiff base product of condensation of *S*-benzyl dithiocarbamate and 2-acetylpyridine, has a bridged dimeric Cu₂Cl₂(L)₂ structure with distorted square pyramidal geometry. Each of the two copper atoms is five-coordinated to one of the two tridentate chelating ligands and both bridging chlorine atoms. To define structure–activity relationships, we investigated the bioactivity of related metal–ligand complexes derived from different metal(II) atoms and different ligands. Complexation of the NSC 295642 ligand with Zn(II) or Ni(II), delivered as metal(II) chloride salts under conditions identical to those used for preparation of the original Cu(II) complex, instead results in distorted octahedral bis-chelate structures, where a single metal atom is six-coordinated to two ligands. The Zn(L)₂ complex possesses a potency similar to that of the Cu₂Cl₂(L)₂ complex, while the Ni(L)₂ has no antimigratory activity at all. We carried out density functional theory calculations to obtain the electronic ground state geometry of the complexes, both in vacuum and implicit water solvent. The X-ray crystal and energy-minimized structures are very similar and exhibit a *transoid* orientation of the *S*-benzyl groups relative to the central metal-coordinated rings for both of the bioactive Cu₂Cl₂(L)₂ and Zn(L)₂ complexes, despite their different coordination geometries. In contrast, the biologically inactive Ni(L)₂ complex adopts a *cisoid* conformation. Varying the ligand structure, we found that hydrophobic *S*-alkylaryl groups are required for activity. Complexes with a simple *S*-methyl group, *S*-benzyl groups with polar substitutions or a carboxylated pyridine ring exhibit dramatically reduced activity. We tested the most potent metal–ligand complex in a number of cancer cell lines and found cell-type selectivity in its effect on cell motility. Collectively, these results suggest that a two-ligand structure with bulky nonpolar *S*-substituents in a *transoid* conformation is important for the antimigratory activity of these metal–ligand complexes.

© 2008 Published by Elsevier Ltd.

Complexes of metals and organic ligands are becoming recognized as useful probes for biological research and as potential therapeutic agents.¹ Certain metal–ligand complexes can form structures that resemble traditional drug-like organic molecules. In these complexes, the metal serves to coordinate the organic ligand, thus potentially generating an organic pharmacophore whose structure is determined by the structure imposed upon the ligand through chelation of the metal. A number of biologically active metal–ligand complexes of this kind have been identified.¹

Keywords: Cell migration inhibitors; Metal–ligand complexes; Structure–activity relationships.

* Corresponding author. Tel.: +1 860 486 6645; fax: +1 860 486 2981; e-mail: gabriel.fenteany@uconn.edu

[†] Present address: Department of Medicinal Chemistry, National Institute of Pharmaceutical Education and Research, SAS Nagar, Punjab 160062, India.

Cell migration is a basic biological process involved in a range of normal and pathological events, including wound healing, embryonic and tissue development, immune function and inflammation, angiogenesis and tumor metastasis. We screened the National Cancer Institute (NCI) Diversity Set collection of compounds in a cell migration assay based on the closure of scratch wounds by Madin–Darby canine kidney (MDCK) epithelial cell sheets in culture, a system we have previously used to identify new agents with antimigratory activity.^{2–4} Here we report that NSC 295642 (Fig. 1), a Cu(II) complex of the Schiff base product of condensation of *S*-benzyl dithiocarbamate and 2-acetylpyridine, is a potent inhibitor of cell motility with an IC₅₀ of 93 nM (Table 1). This compound has also been reported to weakly inhibit the dual specificity phosphatase Cdc25.⁵ Other complexes of the same ligand have antifungal⁶ and antiamebic activities.^{7,8}

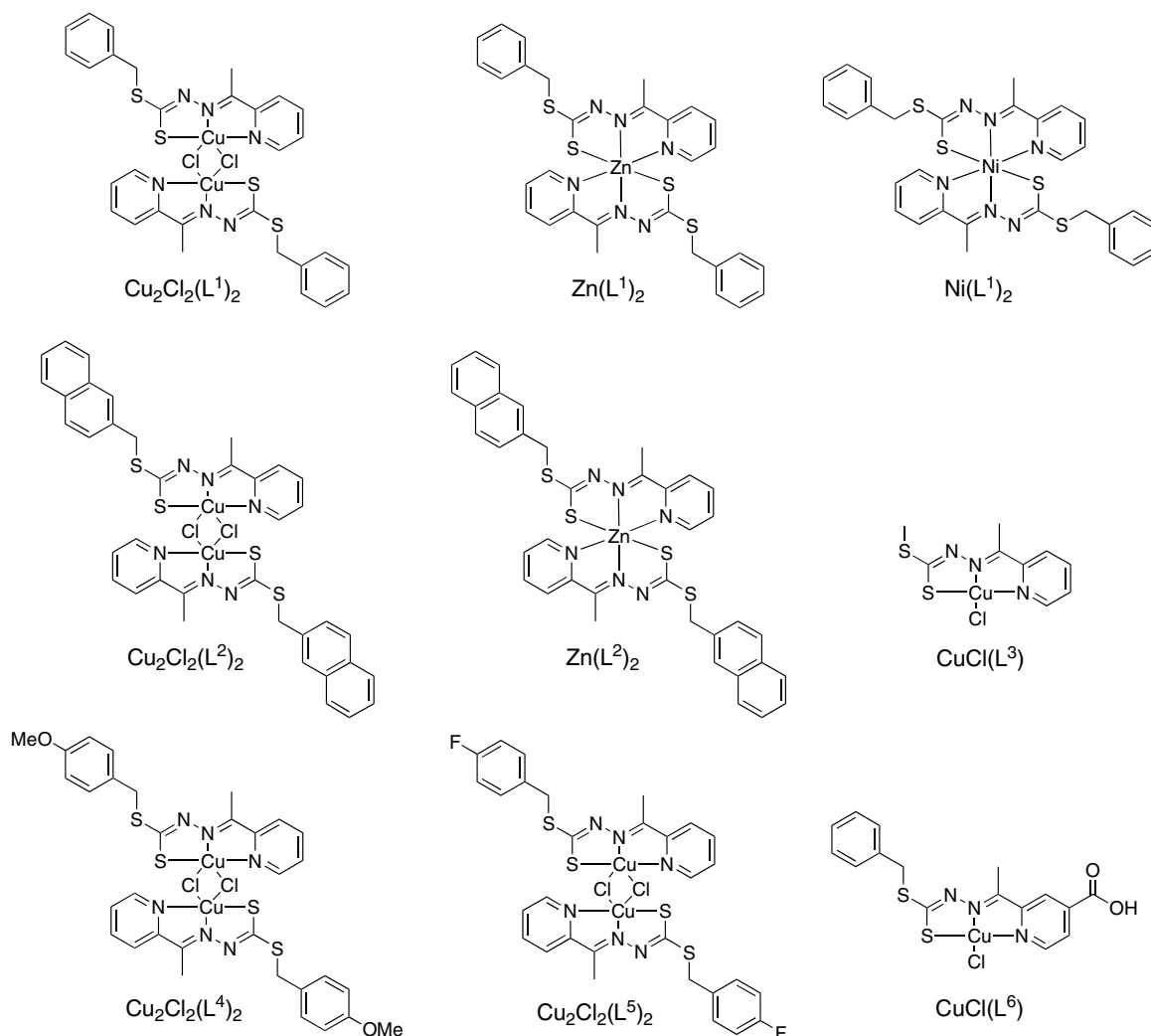


Figure 1. Metal(II)–ligand complexes synthesized and tested for antimigratory activity.

Table 1. Antimigratory activity of NSC 295642 and its analogs

Compound	IC ₅₀ ^a (nM)	MIC ^b (nM)	% of control ^c	MLC ^d (nM)
Cu ₂ Cl ₂ (L ¹) ₂	93	75	34	2000
Zn(L ¹) ₂	238	50	56	1000
Ni(L ¹) ₂	NA ^e	NA	NA	1000
Cu ₂ Cl ₂ (L ²) ₂	58	30	29	1000
Zn(L ²) ₂	181	100	44	1000
CuCl(L ³)	NA	NA	NA	3000
Cu ₂ Cl ₂ (L ⁴) ₂	T ^f	T	—	500
Cu ₂ Cl ₂ (L ⁵) ₂	T	T	—	500
CuCl(L ⁶)	NA	NA	NA	2000

^a Concentration for half-maximal inhibition of wound closure at 24-h post-wounding.

^b Minimum inhibitory concentration (lowest concentration that showed statistically significant inhibition of wound closure at 24-h post-wounding, based on unpaired two-tailed Student's *t*-test with *p* < 0.05).

^c Degree of inhibition of wound closure at 24-h post-wounding expressed as a function of percent of parallel controls at maximal subtoxic concentrations. The smaller the value, the more bioactive the compound is.

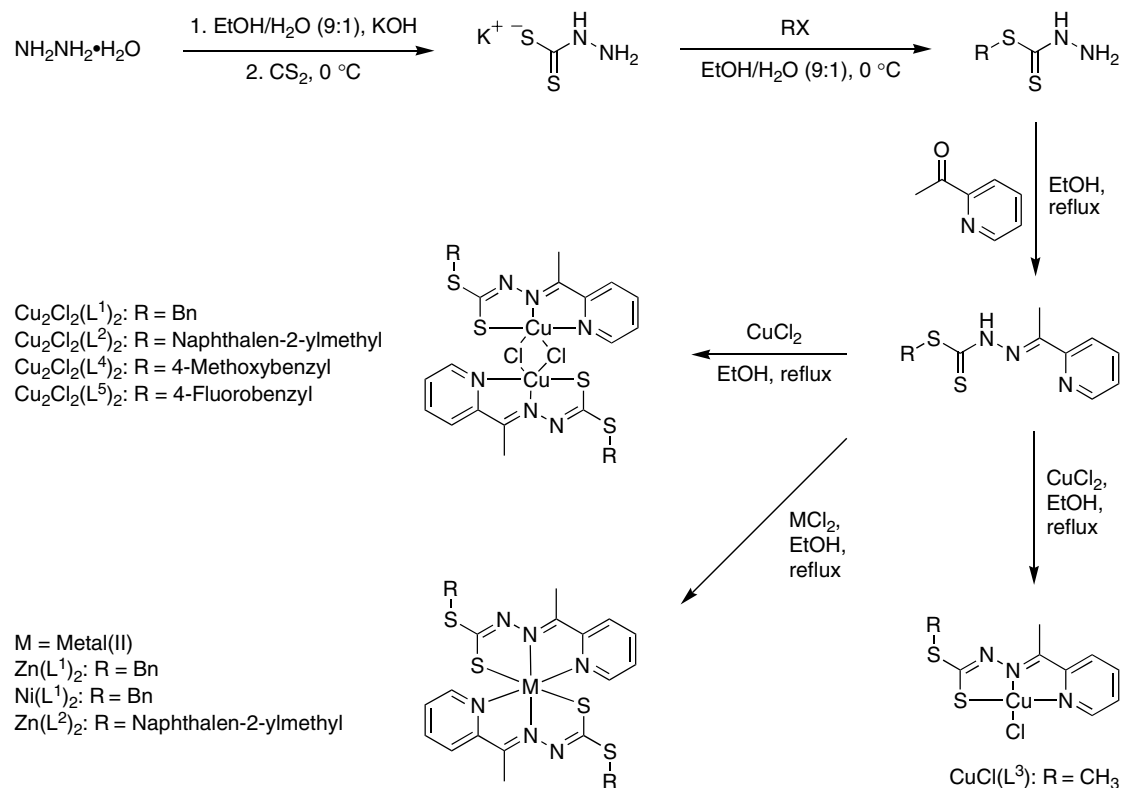
^d Minimum lethal concentration (as determined by the Trypan blue dye exclusion assay).

^e No activity; not significantly different from control.

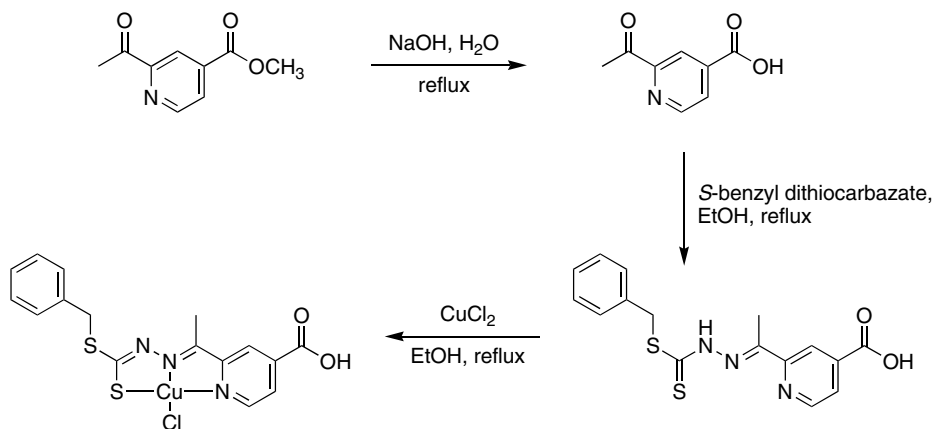
^f Cytotoxic without any subtoxic antimigratory activity.

We prepared NSC 295642 and found the compound synthesized in our laboratory to have biological activity that was indistinguishable from the sample from NCI. This molecule and the other complexes described below

were prepared by synthesis of the different ligands and complexation with metal(II), delivered as CuCl₂, ZnCl₂ or NiCl₂, as shown in Schemes 1 and 2.^{9–13} Although NSC 295642 is depicted as a single-ligand structure of



Scheme 1. Synthesis of metal(II) complexes of Schiff base products of condensation of *S*-alkyl dithiocarbazates with 2-acetylpyridine (L^1 to L^5 complexes).



Scheme 2. Synthesis of $\text{CuCl}(\text{L}^6)$ complex.

basic formula $\text{CuCl}(\text{L}^1)$ in the NCI's Developmental Therapeutics Program database, both the NCI sample and the material we prepared are dimers. The complex has a basic formula of $\text{Cu}_2\text{Cl}_2(\text{L}^1)_2$ and is composed of two five-coordinate copper atoms each chelated by one of the tridentate ligands and bridged by the two chlorine atoms (Fig. 1), based on LC-MS¹³ and X-ray crystallography.¹⁴

We synthesized related molecules to define structure-activity relationships, varying both the chelated metal and structure of the ligand (Schemes 1 and 2).^{9–13} Complexation of the NSC 295642 ligand with Zn(II) also resulted in a two-ligand complex (Fig. 1). However, the

ligands form a bis-chelate structure with a single six-coordinate zinc atom, a complex with a basic formula of $\text{Zn}(\text{L}^1)_2$, as determined by LC-MS¹³ and X-ray crystallography.¹⁴ Since Zn(II) is diamagnetic, unlike the paramagnetic Cu(II), we acquired ¹H and ¹³C NMR spectra for the $\text{Zn}(\text{L}^1)_2$ complex.¹³ The NMR data also suggest a stable $\text{Zn}(\text{L}^1)_2$ structure, with diastereotopic *S*-benzyl methylene protons, and are not consistent with a mixture of dissociated single-ligand $\text{Zn}(\text{L}^1)$ complex and free ligand; furthermore, the free ligand displays a distinct NMR profile.¹³ In addition, a complex of Zn(II) with an almost identical ligand that simply lacks the L^1 methyl group (nor- L^1) also has a two-ligand structure, with the same (N,N,S)₂ donor set and basic coordi-

nation geometry as $Zn(L^1)_2$, and does not dissociate in DMSO, based on conductivity measurements.¹⁵

Despite its difference in coordination geometry from the $Cu_2Cl_2(L^1)_2$ complex, the $Zn(L^1)_2$ complex is nonetheless also highly potent as an inhibitor of cell migration, with an IC_{50} of 238 nM (Table 1). Complexation of the NSC 295642 ligand with Ni(II) also yielded a six-coordinate complex with the basic formula $Ni(L^1)_2$, as revealed by LC-MS¹³ and X-ray crystallography.¹⁴ In contrast to the other NSC 295642 ligand-based complexes, however, $Ni(L^1)_2$ is completely devoid of any subtoxic activity in our wound closure experiments, although it does become cytotoxic at $\geq 1 \mu M$.

The bioactivity of the Cu(II)–ligand or Zn(II)–ligand complexes appears to depend on an intact structure that is already formed upon treatment of the cells. Treatment with non-complexed ligand alone (5 μM), on the one hand, or $CuCl_2$ or $ZnCl_2$ (or $NiCl_2$) alone (50 μM), on the other, has no effect on cells (data not shown). Therefore, the bioactivity cannot be attributed to the products of possible complete dissociation of the bioactive complexes. We cannot definitively rule out, however, that the $Cu_2Cl_2(L^1)_2$ and $Zn(L^1)_2$ complexes could dissociate under the conditions of cell culture into single-ligand complexes that might possess bioactivity, for example, two single-ligand complexes in the case of $Cu_2Cl_2(L^1)_2$ and a single-ligand complex and inactive free ligand in the case of $Zn(L^1)_2$. However, the $Cu_2Cl_2(L^1)_2$ and $Zn(L^1)_2$ complexes appear stable under different analytical conditions,^{13,14} as does the Zn(II) complex of nor- L^1 .¹⁵

We generated analogs where the original *S*-benzyl group of NSC 295642 was substituted with other groups. An *S*-naphthalen-2-ylmethyl group in the ligand resulted in slightly better bioactivity for the Cu(II) and Zn(II) complexes [$Cu_2Cl_2(L^2)_2$ and $Zn(L^2)_2$], with IC_{50} values of 58 and 181 nM, respectively. Fig. 2a shows the progress of wound closure in MDCK cell monolayers in the presence of the most potent of the metal–ligand complexes tested, $Cu_2Cl_2(L^2)_2$. In contrast, an *S*-methyl substituent yielded a complex with a single-ligand structure [$CuCl(L^3)$] and no subtoxic activity. Ligands with more polar substituents, *S*-4-methoxybenzyl and *S*-4-fluorobenzyl, also resulted in complexes, $Cu_2Cl_2(L^4)_2$ and $Cu_2Cl_2(L^5)_2$, respectively, that were devoid of subtoxic activity. Finally, an analog was generated with a carboxyl group in the *para* position of the pyridine ring [$CuCl(L^6)$]. The complex has a single-ligand structure, as with ligand L^3 , and has no subtoxic activity. While we cannot rule out that single-ligand structures derived from different ligands could also potentially be bioactive, among the compounds examined, all of the bioactive molecules have a two-ligand structure.

Since $Cu_2Cl_2(L^2)_2$ was the most potent inhibitor of cell migration (Table 1), we evaluated its biological activity in a number of cancer cell lines as well, specifically human breast carcinoma (T47D and BT20) and human colorectal carcinoma (HCT116) cell lines. We employed scratch-wound assays similar to that used with MDCK

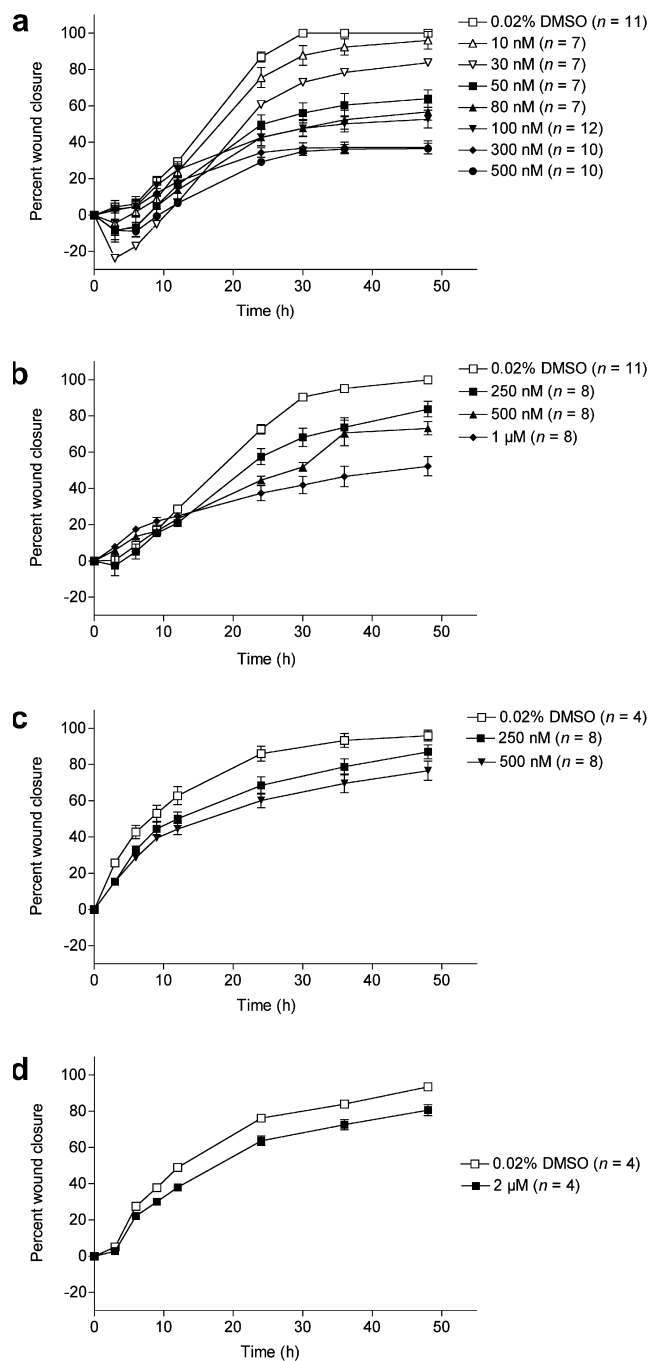


Figure 2. Progress of wound closure in different cell monolayers as a function of concentration of $Cu_2Cl_2(L^2)_2$. Cell lines: (a) MDCK epithelial cells; (b) T47D human breast carcinoma cells; (c) BT20 human breast carcinoma cells; (d) HCT116 human colorectal carcinoma cells.

cell monolayers. MDCK cells are clearly the most sensitive of the cell lines to the $Cu_2Cl_2(L^2)_2$ (Fig. 2a). The compound displays antimigratory activity in T47D cells (Fig. 2b), less in BT20 cells (Fig. 2c), and very little in HCT116 cells (Fig. 2d). The compound thus appears selective for certain cell lines.

Finally, we sought to understand why NSC 295642 [$Cu_2Cl_2(L^1)_2$] and the corresponding Zn(II) complex [$Zn(L^1)_2$] were bioactive, while the corresponding Ni(II)

complex $[\text{Ni}(\text{L}^1)_2]$ was not. We therefore compared the X-ray crystal structures of these three complexes.¹⁴ The bioactive $\text{Cu}_2\text{Cl}_2(\text{L}^1)_2$ possesses a distorted square

pyramidal coordination geometry, while both the bioactive $\text{Zn}(\text{L}^1)_2$ complex and inactive $\text{Ni}(\text{L}^1)_2$ complex have distorted octahedral coordination geometries (Fig. 3).

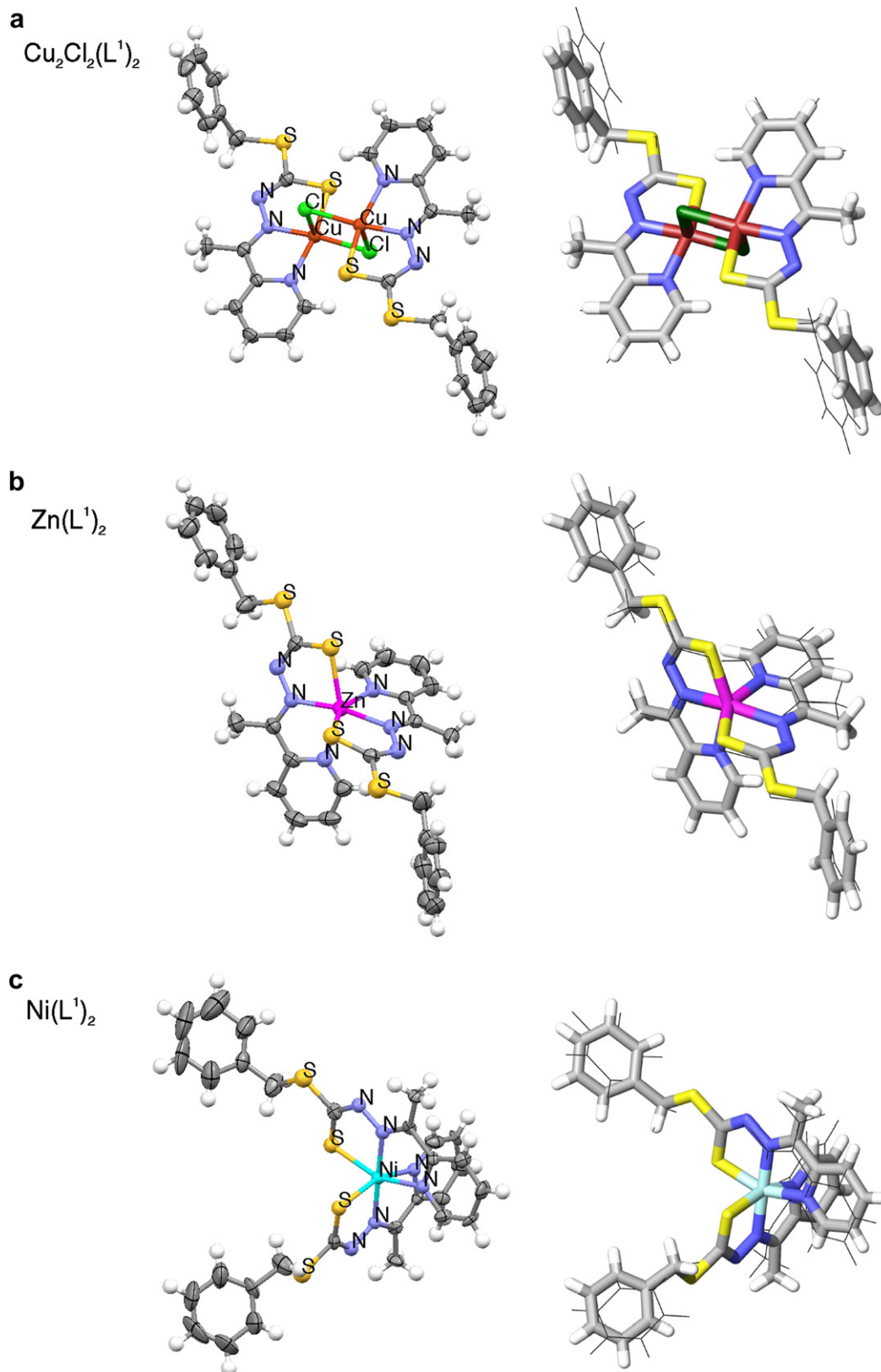


Figure 3. X-ray crystal and energy-minimized structures of metal(II)-ligand complexes. X-ray crystal structures are shown, on the left, as thermal ellipsoid plots (at 50% probability level) and, on the right, as capped stick models superimposed over wire models of structures derived from DFT energy-minimization calculations for $\text{Cu}_2\text{Cl}_2(\text{L}^1)_2$, $\text{Zn}(\text{L}^1)_2$, and $\text{Ni}(\text{L}^1)_2$ complexes.

Clearly, differences in coordination geometry cannot explain the differences in bioactivity between the complexes.

The $\text{Cu}_2\text{Cl}_2(\text{L}^1)_2$ and $\text{Zn}(\text{L}^1)_2$ complexes do, however, share a common conformational feature. Both these bioactive complexes exhibit a *transoid* orientation of the sulfides with respect to the central metal-coordinated rings; note the S–C bonds of the two *S*-benzyl groups relative to the S–C bonds of the coordinated rings (Fig. 3a and b). The $\text{Zn}(\text{II})$ complex of nor- L^1 also adopts a *transoid* conformation.¹⁵ The *S*-benzyl groups of the $\text{Cu}_2\text{Cl}_2(\text{L}^1)_2$ and $\text{Zn}(\text{L}^1)_2$ complexes point in opposite directions, despite the difference in metal stoichiometry and coordination geometry. In contrast, the biologically inactive $\text{Ni}(\text{L}^1)_2$ complex possesses a *cisoid* orientation of the sulfides relative to the $\text{Ni}(\text{II})$ -coordinated rings, with the *S*-benzyl groups in closer proximity to one another (Fig. 3c).

Energy minimization via density functional theory (DFT) calculations,^{16,17} both in vacuum and implicit water solvent, resulted in structures that were substantially similar to the X-ray crystal structures (Fig. 3). The DFT calculations thus suggest that the conformations the complexes assume as crystals are likely to be close to the lowest-energy conformations they would adopt in solution. We calculated that the *transoid* conformation of $\text{Cu}_2\text{Cl}_2(\text{L}^1)_2$, for example, would be 7.6 kcal/mol more stable than the *cisoid* conformation. Interestingly, there is an even stronger preference in silico for a *transoid* conformation when the *S*-benzyl groups of $\text{Cu}_2\text{Cl}_2(\text{L}^1)_2$ are replaced with *O*-benzyl groups, with *transoid* favored over *cisoid* by 12.3 kcal/mol.

The data presented here imply that the pharmacophore of NSC 295642 and related metal–ligand complexes is at least in part formed by hydrophobic *S*-alkylaryl groups that adopt a *transoid* orientation relative to the central metal-coordinating rings, which affects the way the hydrophobic moieties project from the core structures. It is possible that each hydrophobic group fits into a hydrophobic pocket on a target protein when the groups are projected far enough away from one another, as in the *transoid* $\text{Cu}_2\text{Cl}_2(\text{L}^1)_2$ and $\text{Zn}(\text{L}^1)_2$ complexes. In contrast, the two *S*-benzyl groups in the *cisoid* $\text{Ni}(\text{L}^1)_2$ complex are closer together, and so steric hindrance may prevent a target protein from binding either group.

Acknowledgments

This work was supported by grants from the National Institutes of Health (R01GM077622) and the American Cancer Society (RSG-02-250-01-DDC) to G.F. We thank the NCI for providing its Diversity Set collection of compounds and an additional sample of NSC 295642, D.J. Wink for technical assistance and C. Brückner and S.C. Burdette for critical reading of the manuscript.

References and notes

- Meggens, E. *Curr. Opin. Chem. Biol.* **2007**, *11*, 287.
- Mc Henry, K. T.; Ankala, S. V.; Ghosh, A. K.; Fenteany, G. *ChemBioChem* **2002**, *11*, 1105.
- Zhu, S.; Mc Henry, K. T.; Lane, W. S.; Fenteany, G. *Chem. Biol.* **2005**, *12*, 981.
- Kahsai, A. W.; Zhu, S.; Wardrop, D. J.; Lane, W. S.; Fenteany, G. *Chem. Biol.* **2006**, *13*, 973.
- Vogt, A.; Cooley, K. A.; Brisson, M.; Tarpley, M. G.; Wipf, P.; Lazo, J. S. *Chem. Biol.* **2003**, *10*, 733.
- Hossain, M. E.; Alam, M. N.; Ali, M. A.; Nazimuddin, M.; Smith, F. E.; Hynes, R. C. *Polyhedron* **1995**, *15*, 973.
- Bharti, N.; Maurya, M. R.; Naqvi, F.; Azam, A. *Bioorg. Med. Chem. Lett.* **2000**, *10*, 2243.
- Neelam, B.; Mannar, M.; Fehmida, N.; Alok, B.; Sudha, B.; Amir, A. *Eur. J. Med. Chem.* **2000**, *35*, 481.
- Das, M.; Livingstone, S. E. *Inorg. Chim. Acta* **1976**, *19*, 5.
- Ali, M. A.; Tarafder, M. T. H. *J. Inorg. Nucl. Chem.* **1977**, *39*, 1785.
- Hossain, M. E.; Begum, J.; Alam, M. N.; Nazimuddin, M.; Ali, M. A. *Transition Met. Chem.* **1993**, *18*, 497.
- Mikel, C.; Potvin, P. G. *Polyhedron* **2002**, *21*, 49.
- A mixture of each prepared *S*-alkyl dithiocarbazate and 2-acetylpyridine (or 2-acetylisonicotinic acid in the case of synthesis of L^6) in a 1:1 molar ratio in absolute ethanol was boiled for 2 h.^{9–11} Precipitates of the Schiff bases were deposited from the mixture upon cooling in ice. The precipitates were filtered off, washed with ice-cold ethanol, and dried in vacuo (yield = 50–80%). L^6 was prepared by hydrolysis of the methyl ester of methyl 2-acetylisonicotinate,¹² followed by reaction with *S*-benzyl dithiocarbazate as above. To prepare each metal(II) complex, an equimolar mixture of Schiff base ligand and CuCl_2 , ZnCl_2 or NiCl_2 in absolute ethanol was heated at 60 °C (oil-bath temperature) for 10 min. Precipitates of each complex formed upon cooling to room temperature. The precipitates were filtered off, washed with ice-cold ethanol, crystallized in acetonitrile, and dried in vacuo (yield = 40–54%). NMR spectra were acquired for all free ligands, as well as the $\text{Zn}(\text{L}^1)_2$ and $\text{Ni}(\text{L}^1)_2$ complexes. (Note: The four pyridyl protons appeared duplicated by ^1H NMR for the free ligands L^1 , L^2 , and L^3 in CDCl_3 , possibly as a consequence of thione–thiol tautomerism; more directly consistent with this possibility, we observed broadened and weakened NH proton signal, although we were unable to clearly identify SH proton resonance.) LC-ESIMS was performed in methanol.
 L^1 ligand. ^1H NMR (400 MHz, CDCl_3) δ 9.97 (br s, 1H, NH), 8.76 (dd, J = 1.6 Hz, 4.0 Hz, 1H, Py-H), 8.62 (d, J = 5.2 Hz, 1H, Py-H), 8.18 (d, J = 8.8 Hz, 1H, Py-H), 7.90 (dt, J = 1.6 Hz, 8.0 Hz, 1H, Py-H), 7.75 (t, J = 7.6 Hz, 1H, Py-H), 7.59 (d, J = 8.4 Hz, 1H, Py-H), 7.26–7.44 (m, 7H, Ph-H and Py-H), 4.55 (s, 2H, CH_2), 2.42 (d, J = 9.5 Hz, 3H, CH_3). ^{13}C NMR (100 MHz CDCl_3) δ 200.05, 199.36, 153.80, 147.99, 137.83, 137.38, 135.74, 129.50 (2C), 129.46, 129.21, 128.67 (2C), 128.54, 127.61, 127.31, 124.47, 124.07, 121.42, 39.68, 38.92, 22.11, 11.43.
 $\text{Zn}(\text{L}^1)_2$ complex. ^1H NMR (400 MHz, CDCl_3) δ 7.90–7.92 (m, 1H, Py-H), 7.80 (dt, J = 1.6 Hz, 6.3 Hz, 1H, Py-H), 7.68–7.69 (d, J = 6.4 Hz, 1H, Py-H), 7.42–7.44 (m, 2H, Ph-H and Py-H), 7.21–7.31 (m, 4H, Ph-H), 4.58 (d, J = 10.7 Hz, 1H, CH_2), 4.47 (d, J = 10.7 Hz, 1H, CH_2), 2.72 (s, 3H, CH_3). ^{13}C NMR (100 MHz, CDCl_3) δ 191.50, 152.84, 149.52, 147.07, 138.70, 137.98, 129.17 (2C), 128.29 (2C), 126.77, 125.55, 122.30, 36.72, 14.34.
 $\text{Ni}(\text{L}^1)_2$ complex. ^1H NMR (400 MHz, CDCl_3) δ 8.66 (d, J = 5.6 Hz, 1H, Py-H) 7.88–7.92 (m, 2H, Py-H), 7.29–7.42 (m, 6H, Ph-H and Py-H), 4.36 (s, 2H, CH_2), 2.30 (s, 3H, CH_3).

ESIMS for L¹ complexes. Cu₂Cl₂(L¹)₂: calcd 760.9 [M–Cl]⁺, found 760.7. Zn(L¹)₂: calcd 687.0 [M+Na]⁺; found: 686.8. Ni(L¹)₂: calcd 681.0 [M+Na]⁺; found: 680.9.

L² ligand. ¹H NMR (400 MHz, CDCl₃) δ 9.94 (br s, 1H, NH), 8.75 (d, *J* = 4.0 Hz, 1H, Py-H), 8.56 (d, *J* = 4.0 Hz, 1H, Py-H), 8.11 (d, *J* = 8.0 Hz, 1H, naphthyl-H), 7.75–7.89 (m, 6H, naphthyl-H and Py-H), 7.63 (dt, *J* = 1.8 Hz, 6.2 Hz, 1H, Py-H), 7.25–7.57 (m, 5H, naphthyl-H and Py-H), 4.72 (s, 2H, CH₂), 2.42 (d, *J* = 20 Hz, 3H, CH₃).

ESIMS for L² complexes. Cu₂Cl₂(L²)₂: calcd 860.9 [M–Cl]⁺; found: 860.9. Zn(L²)₂: calcd 765.1 [M+H]⁺; found: 764.9.

L³ ligand. ¹H NMR (400 MHz, CDCl₃) δ 10.04 (br s, 1H, NH), 8.70 (dt, *J* = 1.6 Hz, 4.8 Hz, 1H, Py-H), 8.57 (dt, *J* = 1.6 Hz, 4.8 Hz, 1H, Py-H), 8.16 (d, *J* = 8.0 Hz, 1H, Py-H), 7.90 (t, *J* = 8.0 Hz, 1H, Py-H), 7.69 (dd, *J* = 1.6 Hz, 8.0 Hz, 1H, Py-H), 7.57 (d, *J* = 8.0 Hz, 1H, Py-H), 7.33–7.36 (m, 1H, Py-H), 7.26–7.29 (m, 1H, Py-H), 2.64 (d, *J* = 10.6 Hz, 3H, CH₃), 2.42 (d, *J* = 6.5 Hz, 3H, CH₃).

ESIMS for L³ complex. CuCl(L³): calcd 608.8 [M]⁺; found: 608.8.

L⁴ ligand. ¹H NMR (400 MHz, DMSO-*d*₆) δ 12.58 (s, 1H, NH), 8.62 (d, *J* = 4.1 Hz, 1H, Py-H), 8.01 (d, *J* = 8.1 Hz, 1H, Py-H), 7.85 (dt, *J* = 1.8 Hz, 6.0 Hz, 1H, Py-H), 7.44 (dt, *J* = 1.1 Hz, 4.8 Hz, 1H, Py-H), 7.35 (d, *J* = 8.7 Hz, 2H, Ph-H), 6.90 (d, *J* = 8.7 Hz, 2H, Ph-H), 4.44 (d, 2H, CH₂), 3.75 (s, 3H, OCH₃), 3.32 (s, 3H, CH₃).

ESIMS for L⁴ complex. Cu₂Cl₂(L⁴)₂: calcd 820.9 [M–Cl]⁺; found: 820.8.

L⁵ ligand. ¹H NMR (400 MHz, DMSO-*d*₆) δ 12.66 (s, 1H, NH), 8.62 (d, *J* = 4.88 Hz, 1H, Py-H), 8.03 (d, *J* = 6.64 Hz, 1H, Py-H), 7.88 (dt, *J* = 4.6 Hz, 10.9 Hz, 1H, Py-H), 7.45–7.50 (m, 3H, Ph-H and Py-H), 7.14–7.19 (m, 2H, Ph-H), 4.50 (s, 2H, CH₂), 2.33 (s, 3H, CH₃).

ESIMS for L⁵ complex. Cu₂Cl₂(L⁵)₂: calcd 796.8 [M–Cl]⁺; found: 796.9.

L⁶ ligand. ¹H NMR (400 MHz, acetone-*d*₆) δ 10.64 (s, 1H, COOH), 8.79 (d, *J* = 8.0 Hz, 1H, Py-H), 8.66 (s, 1H, NH), 7.90 (dd, *J* = 1.2 Hz, 3.53 Hz, 1H, Py-H), 7.46 (d, *J* = 7.7 Hz, 2H, Ph-H), 7.26–7.34 (m, 4H, Ph-H and Py-H), 4.54 (s, 2H, CH₂), 2.62 (s, 3H, CH₃).

ESIMS for L⁶ complex. CuCl(L⁶): calcd 440.9 [M]⁺; found: 440.8.

14. Crystallographic data for Cu₂Cl₂(L¹)₂, Zn(L¹)₂, and Ni(L¹)₂ have been deposited with the Cambridge Crystallographic Data Centre as supplementary publication numbers CCDC-660437, -660438, and -660439, respectively. These data can be obtained free of charge via www.ccdc.cam.ac.uk/cgi-bin/catreq.cgi, or by emailing data_request@ccdc.cam.ac.uk, or by contacting The Cambridge Crystallographic Data Centre, 12, Union Road, Cambridge CB2 1EZ, UK; fax: +44 1223 336033.
15. Tarafder, M. T. H.; Kasbollah, A.; Crouse, K. A.; Ali, A. M.; Yamin, B. M.; Fun, H.-K. *Polyhedron* **2001**, *20*, 2363.
16. Starting from the coordinates of the X-ray crystal structures, DFT calculations were performed using the Becke-3-*Lee-Yang-Parr* hybrid density functional to predict the ground electronic state geometry. We employed the basis set LANL2DZ for the transition metals, which includes electron core potential, and 6-31G(d) for the rest of the atoms. Energy minimization for each of the three compounds was carried out in both vacuum and in the presence of implicit water solvent. The program Gaussian 03¹⁷ was used for all DFT calculations.
17. Frisch, M. J.; Trucks, G. W.; Schlegel, H. B.; Scuseria, G. E.; Robb, M. A.; Cheeseman, J. R.; Montgomery, Jr., J. A.; Vreven, T.; Kudin, K. N.; Burant, J. C.; Millam, J. M.; Iyengar, S. S.; Tomasi, J.; Barone, V.; Mennucci, B.; Cossi, M.; Scalmani, G.; Rega, N.; Petersson, G. A.; Nakatsuji, H.; Hada, M.; Ehara, M.; Toyota, K.; Fukuda, R.; Hasegawa, J.; Ishida, M.; Nakajima, T.; Honda, Y.; Kitao, O.; Nakai, H.; Klene, M.; Li, X.; Knox, J. E.; Hratchian, H. P.; Cross, J. B.; Bakken, V.; Adamo, C.; Jaramillo, J.; Gomperts, R.; Stratmann, R. E.; Yazyev, O.; Austin, A. J.; Cammi, R.; Pomelli, C.; Ochterski, J. W.; Ayala, P. Y.; Morokuma, K.; Voth, G. A.; Salvador, P.; Dannenberg, J. J.; Zakrzewski, V. G.; Dapprich, S.; Daniels, A. D.; Strain, M. C.; Farkas, O.; Malick, D. K.; Rabuck, A. D.; Raghavachari, K.; Foresman, J. B.; Ortiz, J. V.; Cui, Q.; Baboul, A. G.; Clifford, S.; Cioslowski, J.; Stefanov, B. B.; Liu, G.; Liashenko, A.; Piskorz, P.; Komaromi, I.; Martin, R. L.; Fox, D. J.; Keith, T.; Al-Laham, M. A.; Peng, C. Y.; Nanayakkara, A.; Challacombe, M.; Gill, P. M. W.; Johnson, B.; Chen, W.; Wong, M. W.; Gonzalez, C.; and Pople, J. A. *Gaussian 03*, Revision B.05; Gaussian, Inc.: Wallingford CT, 2004.